CCFE
CULHAM CENTRE FOR FUSION ENERGY

UK Atomic Energy Authority

UKAEA-CCFE-PR(18)79

Lee Packer, P. Batistoni, S. C. Bradnam, S. Conroy, Z. Ghani, M. R. Gilbert, E. Laszynska, I. Lengar, C.R.Nobs, M. Pillon, S. Popovichev, P. Raj, I.E. Stamatelatos, T. Vasilopoulou, A. Wojcik-Gargula, R. Worrall and JET Contributors

Neutron spectrum determination at the ITER material irradiation stations at JET

Neutron spectrum determination at the ITER material irradiation stations at JET

Lee Packer, P. Batistoni, S. C. Bradnam, S. Conroy, Z. Ghani, M. R. Gilbert, E. Laszynska, I. Lengar, C.R.Nobs, M. Pillon, S. Popovichev, P. Raj, I.E. Stamatelatos, T. Vasilopoulou, A. Wojcik-Gargula, R. Worrall and JET Contributors

This is a preprint of a paper submitted for publication in Fusion Engineering and Design

Neutron spectrum determination at the ITER material irradiation stations at JET

L. W. Packer[a,1], P. Batistoni[b], S. C. Bradnam[a], S. Conroy[h], Z. Ghani[a], M. R. Gilbert[a], E. Łaszyńska[e], I. Lengar[f], C.R.Nobs[a], M. Pillon[b], S. Popovichev[a], P. Raj[h], I.E. Stamatelatos[g], T. Vasilopoulou[g], A. Wójcik-Gargula[d], R. Worrall[a], and JET Contributors[2]

[a] *Culham Centre for Fusion Energy, Culham Science Centre, Abingdon, Oxon, OX14 3DB, UK*
[b] *ENEA - Department of Fusion and Technology for Nuclear Safety and Security via E. Fermi 45, 00044 Frascati (Rome), Italy*
[c] *VR Association, Uppsala University, Department of Physics and Astronomy, PO Box 516, SE-75120 Uppsala, Sweden*
[d] *Institute of Nuclear Physics, Polish Academy of Sciences, PL-31-342 Krakow, Poland*
[e] *Institute of Plasma Physics and Laser Microfusion, 01-497 Warsaw, Poland*
[f] *Reactor Physics Department, Jožef Stefan Institute, Jamova cesta 39, SI-1000 Ljubljana, Slovenia*
[g] *Institute of Nuclear and Radiological Sciences, Technology, Energy and Safety, NCSR Demokritos, Athens, 15310, Greece*
[h] *Karlsruhe Institute of Technology (KIT), Hermann-von-Helmholtz Platz 1, 76344 Eggenstein-Leopoldshafen, Germany*

Abstract

This paper reports new activities conducted as part of the JET technology programme under the WP-JET3 ACT sub-project collaboration. The aim of the sub-project is to take advantage of the significant 14 MeV neutron fluence expected during JET operations to irradiate samples of materials that will be used in the manufacturing of main ITER tokamak components. Here, experimental measurements of dosimetry foil activity following irradiation in JET irradiation stations have been used as input to a neutron spectrometry unfolding methodology, which is based on an iterative non-linear least squares algorithm, to derive a new neutron spectrum. The new spectra are compared to those originally derived from simulations with the JET fission yield measurements as an input. We conclude that dosimetry foil activation measurements may be used as a complimentary fluence measurement system to that provided by integrated data from fission counter diagnostics, but with an additional benefit that useful spectrum information may be extracted, particularly above 2 MeV.

Keywords: activation, neutronics, fusion

1. Introduction

The experiments that are planned over the next few years at the Joint European Torus (JET), notably including a deuterium-tritium (D–T) experimental phase, are expected to produce large neutron yields, up to 1.7×10^{21} neutrons. The scientific objectives of the experiments are linked with a technology programme, WPJET3, to deliver the maximum scientific and technological return from those operations, with particular emphasis on technology exploitation via the high neutron fluxes predicted in and around the JET machine. The experimental data expected to be retrieved will help to develop and improve the radiation transport and activation simulation capabilities via benchmarking and validation studies in fusion

[1] Corresponding author
[2] See the author list of X. Litaudon et al. 2017 Nucl. Fusion 57 102001

tokamak relevant operational conditions. Significant results have been obtained to date with a focus on relevance to ITER device operations [1]. Nuclear activities that have been performed include the 14 MeV calibration of neutron yield monitors [2], neutronics benchmark experiments [3, 4, 5, 6, 7], nuclear diagnostics and data processing for tritium breeding blankets [8], and activation measurements with supporting analyses for fusion materials [9, 10, 11] for example.

This paper describes some of the latest activities performed under the neutron activation sub-project known as ACT, which has the aim to irradiate a range of real ITER materials in JET experiments and obtain valuable nuclear response benchmark data from those materials. Whilst the main theme of this paper focusses on neutron spectrometry methodology and its application to a large set of dosimetry foil activity measurements obtained in a previous JET campaign, progress towards the next major phase of the sub-project has been made, which is expected to see ITER material samples irradiated in the forthcoming JET deuterium-deuterium (D–D) campaign. A selection of ITER materials samples for use in the sub-project have been collected by Fusion for Energy. These include: poloidal field (PF) coil jacket and toroidal field coil radial closure plate steels, EUROFER 97-3 steel, W and CuCrZr materials from the divertor, Inconel 718, CuCrZr and 316L stainless steel for blanket modules, vacuum vessel forging samples and NbSn toroidal field coil strands, for example. A number of disc sub-samples have now been cut from the bulk material and installed into JET for the D–D campaign expected in late 2018. The newly prepared LTIS assembly, with 26 positions containing the samples, are shown in figure 1 alongside an LTIS assembly used in the experiments discussed in this paper.

Full details of the collaborative work performed in previous experiments, which supported characterisation of the long-term irradiation stations (LTIS) that were used in a 2015–16 JET D–D campaign are detailed in [11]. In summary, 176 high-purity dosimetry foils were irradiated in the LTIS in JET octants 4 and 8. These foils were then disseminated for measurement using high resolution gamma spectrometry

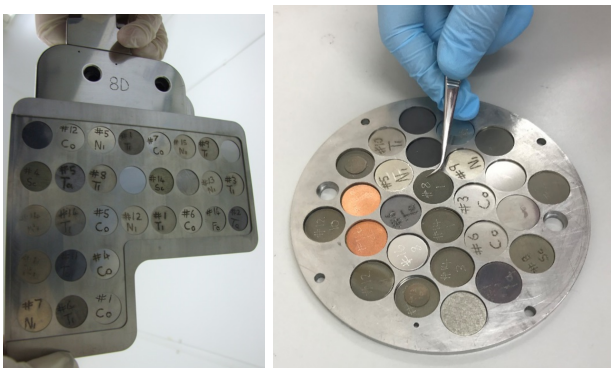

Figure 1: (LHS image)LTIS assembly using on 2015-16 campaign prior to installation and irradiation; (RHS image) New LTIS assembly sample holder containing ITER materials and dosimetry foils prior to installation into JET in 2018.

systems across four EU laboratories. Activity predictions obtained using neutron transport and activation simulations using an updated JET radiation transport model were tested against experimental activity measurements. Conclusions from the previous work showed that the models and simulation approach that was taken is broadly satisfactory for most of the threshold reactions that were studied with an average C/E (calculated over experimental ratio result) of 0.91 ± 0.01 (see figure 2). However, two groups of reactions yielded low C/E, suggesting that parts of the calculated LTIS neutron spectrum can be improved, given that all of these reaction cross sections are considered to be well known and therefore included in the international reactor dosimetry file for fusion and fission (IRDFF). A set of four capture reactions, ^{58}Fe(n,γ)^{59}Fe reaction, ^{45}Sc(n,γ)^{46}Sc reaction, ^{59}Co(n,γ)^{60}Co and ^{181}Ta(n,γ)^{182}Ta reactions all exhibited low C/E values, with a weighted average C/E value across the four sets of measurements of 0.66 ± 0.01, suggesting that the thermal neutron flux is under-predicted in the calculated results. It should be noted that an alternative MCNP model, developed for other aspects of JET nuclear analysis with some differences in Be mass and geometry (for a poloidal limiter component) in the vicinity of the LTIS for example, predicts significantly higher neutron fluences, by approximately a factor of 2, at thermal energies in the LTIS region. The model selected for our reference calculation results presented in this

work is thought to contain a more accurate representation of the Be limiter and total mass. However, we recognise that there may be additional material features that influence the thermal part of the spectrum that we ideally need to capture in an improved model. The deviations between the two models at low energy highlights the relatively large degree of uncertainty in modelling this particular energy region, wheras at energies above 1 MeV the agreement in fluence is within 12%. The ^{89}Y(n,2n)^{88}Y reaction—a high energy threshold sensitive to neutron energies produced in D–T reactions, but not to neutron energies produced via D–D reactions—exhibited a low weighted average C/E value of 0.67 ± 0.03 (see figure 2). This particular reaction is therefore a useful diagnostic of the D–T contribution within the neutron spectrum. One explanation for the low C/E values is that the D–T 14 MeV contribution for the D–D experimental campaign may typically be in the range 0.5–1.5%. In our previous calculations an indicative value of 1% was used, though based on our findings we recognise that this value should be revised. The motivation for this paper follows from these observations and the intention here is to use the experimental results previously obtained, together with an unfolding code and relevant response functions, to revise some energy regions of the calculated LTIS spectrum using an unfolding code in order to obtain improved C/E results across all of the 11 reactions that were measured.

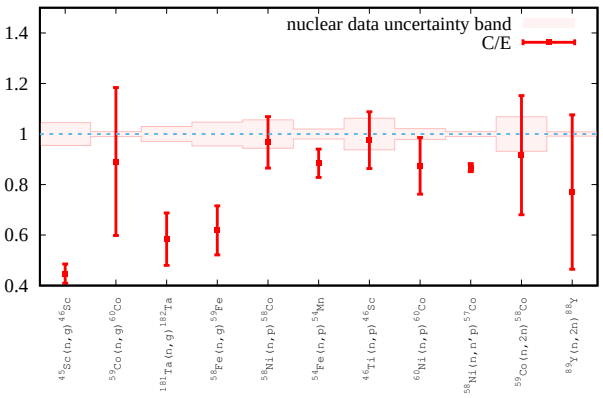

Figure 2: C/E plot for all 11 reactions measured during the experimental campaign. The error bars are the combined measurement uncertainty for each reaction type. The uncertainty band shown is the nuclear data uncertainty for each reaction.

2. Neutron spectrometry methodology

In this work standard inverse problem neutron spectrometry techniques have been performed using methodologies that have been covered extensively in previous literature, for example see [12, 13, 14, 15]. The governing equation is:

$$M_{0n} = \sum_{k=1}^{G_{tot}} R_{n,k}\phi_k$$

and for an activation foil-based measurement M_{0n} is the measured reaction rate for the nth reaction type, $R_{n,k}$ is the response function for the nth reaction type as a function of neutron energy, in G_{tot} energy bins, and ϕ_k is the neutron flux energy spectrum, also in G_{tot} energy bins.

Here, a flexible, modern beta code based on the class of algorithms used in SAND-II [14] and the modified variant GRAVEL [12, 13] has been developed and applied to the data. Two suites of unfolding codes have been developed by UKAEA which are being tested, this work forming part of those tests. A serial code has been written in Python has been used to test the unfolding algorithm and visualise the unfolding process. The other, written in C++, includes a much faster parallelised version which implements a Monte Carlo method for uncertainty propagation and estimation of the condition of the inverse problem given the matrices provided. The main solver used by both of these codes is a non-linear least-squares minimisation method which use an iterative gradient approach to provide an improved solution. An a priori spectrum is used as an initial solution which is evolved to a new spectrum with each iteration. For a set of N reaction rate measurements χ^2 is calculated at each spectrum iteration.

$$\chi^2 = \sum_{n=1}^{N} \left(\frac{M_{0n} - M_n}{\sigma_{M_{0n}}} \right)^2$$

where M_n is the theoretical reaction rate and $\sigma^2_{M_{0n}}$ is the uncertainty in measured reaction rate, M_{0n}.

χ^2 is progressively reduced by a maximum gradi-

ent method, until a solution convergence criteria set by the user is reached. Three termination criteria are available, which may be flexibly set: (i) the χ^2 per degree of freedom is reduced to a user-set target value (normally this is set to 1 or below), (ii) the largest change in flux in an energy bin within the range of interest across an iteration falls below a user-set value, or (iii) a pre-defined number of iterations have been completed.

2.1. Measured reaction rate data and fluence rate corrections

The 176 foil measurements performed by the four laboratories span 11 reaction types. For the nth reaction type an average activity value has been derived, A_n and uncertainty σ_{A_n} at a reference point in time (the end of the JET experimental campaign) by combining individual activity measurements inversely weighted by the square of the corresponding experimental uncertainty. Each A_n is then used to determine a corresponding M_{0n} using

$$M_{0n} = \frac{A_n}{(1 - \exp^{-\lambda_n T})k_n}$$

Because the actual fluence rate during irradiation varied from shot to shot a neutron fluence rate correction factor, k_n, for the nth reaction type has been calculated using FISPACT-II at the end of the full irradiation period and applied to calculate M_{0n}. M_{0n} can be viewed as a time-averaged reaction rate. The irradiation–decay scheme during the JET experimental campaign was complex: a total yield of 2.26×10^{19} neutrons were generated in 3682 experimental JET shots over a period of 446 days. In general, for a series of m distinct irradiation shots, each k_n value may be calculated,

$$k_n = \frac{\sum_{i=1}^{m} \phi_i \left(1 - e^{-\lambda_n \Delta t_i}\right) e^{-\lambda_n T_i}}{\phi \left(1 - e^{-\lambda_n T}\right)}$$

where Δt_i is the time duration of the ith irradiation, T_i is the time from the end of the ith irradiation to the end of the total irradiation period, ϕ_i is the average neutron fluence rate for the ith irradiation period, λ_n is the half life associated with the reaction product nuclide from the nth reaction type and ϕ is the averaged fluence rate across the total irradiation time, T.

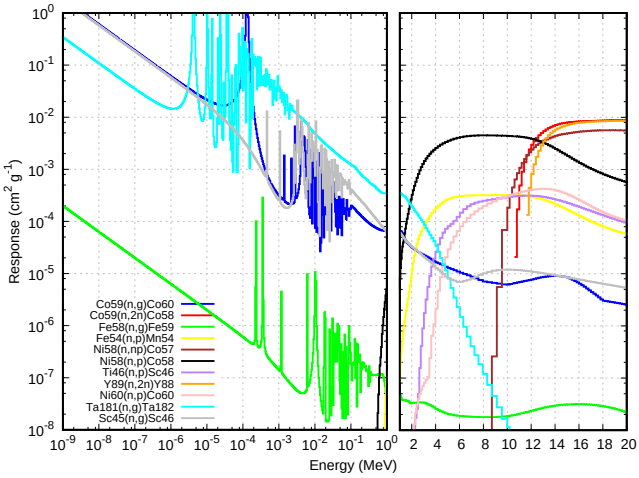

Figure 3: Plot of the 11 calculated response functions associated with the dosimetry foil reactions measured in the experiments. Note the split, logarithmic–linear, x-scale.

For the JET LTIS experimental data set the above quantities have been derived from the measurements. Table 1 shows, for each reaction type, A_n , k_n, M_{0n} and $\sigma_{M_{0n}}$.

2.2. Dosimetry foil response functions

Figure 3 shows a plot of the 11 response functions (RFs) associated with the dosimetry foils used in the experiments. The RFs have been calculated in units of cm^2 g^{-1} using IRDFFv1.05 cross section data libraries, with the exception of the ^{58}Ni(n,n'p)^{57}Co reaction, which does not exist in IRDFFv1.05, and in this case nuclear cross section data from the TENDL-2015 nuclear data library has been used instead. The RFs are calculated in 709 neutron energy groups.

2.3. a priori neutron spectra

The a priori neutron spectrum is as defined in [11] and is used as input to the unfolding code. It was calculated with the Monte Carlo-based radiation transport code MCNP-6.1 [16] with an updated JET MCNP model containing a geometric representation of the long-term irradiation assembly. The purpose of the MCNP simulations were to determine via calculation a representative neutron spectrum within the

Table 1: Table showing reaction type, A_n , k_n, M_{0n} and $\sigma_{M_{0n}}$

Foil	**Reaction type**	A_n	k_n	M_{0n}	$\sigma_{M_{0n}}$
Sc	^{45}Sc(n,γ)^{46}Sc	1.363E+04	1.87	7.472E+03	6.386E+02
Co	^{59}Co(n,2n)^{58}Co	1.097E+02	2.038	5.453E+01	1.403E+01
	^{59}Co(n,γ)^{60}Co	2.197E+03	1.028	1.439E+04	4.735E+03
Ta	^{181}Ta(n,γ)^{182}Ta	2.732E+04	1.596	1.836E+04	3.267E+03
Fe	^{58}Fe(n,γ)^{59}Fe	6.274E+00	2.698	2.328E+00	3.653E-01
	^{nat}Fe(n,x)^{54}Mn; (^{54}Fe(n,p)^{54}Mn)	2.893E+01	1.189	3.871E+01	2.458E+00
Ti	^{nat}Ti(n,x)^{46}Sc; (^{46}Ti(n,p)^{46}Sc)	4.239E+00	1.83	2.375E+00	2.741E-01
Ni	^{nat}Ni(n,x)^{58}Co; (^{58}Ni(n,p)^{58}Co)	1.341E+03	2.04	6.658E+02	7.020E+01
	^{nat}Ni(n,x)^{60}Co; (^{60}Ni(n,p)^{60}Co)	5.271E-01	1.028	3.453E+00	4.437E-01
	^{nat}Ni(n,x)^{57}Co; (^{58}Ni(n,n'p)^{57}Co)	2.874E+01	1.22	3.465E+01	6.363E-01
Y	^{89}Y(n,2n)^{88}Y	8.085E+01	1.631	5.244E+01	2.082E+01

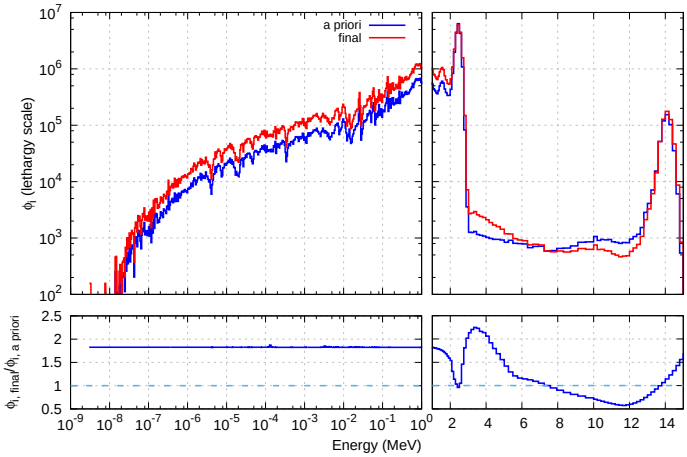

Figure 4: (top section)A-priori neutron spectrum and final spectrum after unfolding. (bottom section) differential ratio plot the two spectra. Note the split, logarithmic–linear, x-scale.

assembly. The a priori spectrum is shown, together with a final unfolded spectrum (explained in the next section), in figure 4.

3. Neutron spectrum unfolding results

Figure 4 shows the a priori spectra and final unfolded spectra following iteration through the unfolding process. Here, the calculation was preformed for 5000 iterations, resulting in a reduction in χ^2 for the final spectrum by a factor of 25 compared to the a priori spectrum.

The total neutron fluence at the LTIS position for the full 446 day irradiation period was calculated using the a priori spectrum, with the KN2 neutron yield measurement as an input, to be 1.06 $\times$ 10^{14} n cm^{-2}. Following the unfolding procedure described above the final calculated spectrum fluence was calculated to be 1.66 $\times$ 10^{14} n cm^{-2}, a factor of 1.57 higher. It is helpful to sub-divide this fluence ratio factor into three distinct energy ranges: 0–2 MeV, 2–10 MeV and above 10 MeV, to broadly understand which parts of the energy spectrum exhibit the largest differences. The ratios are calculated to be 1.82, 1.08 and 1.1 for these energy ranges respectively, showing that the greatest fluence difference between the calculated a priori spectrum and the unfolded spectrum is in the region below 2 MeV, whereas in the higher energy regions above 2 MeV better agreement is obtained, between 8–10%.

The equivalent set of C/E data across all reactions to those shown in figure 2 but with using the final, unfolded spectrum as input is shown in figure 5. One can observe that the level of agreement has significantly improved in comparison to the results shown earlier in figure 2.

4. Discussion and conclusions

Activity measurements of 176 neutron activated dosimetry foils, irradiated in long-term irradiation stations at JET during a JET D–D experimental campaign, have been condensed to a set of 11 distinct reaction rates with associated uncertainties. This data and calculated corresponding response functions have been used together with a neutron spectrometry unfolding methodology, based on an iterative non-linear least squares algorithm, to derive, from

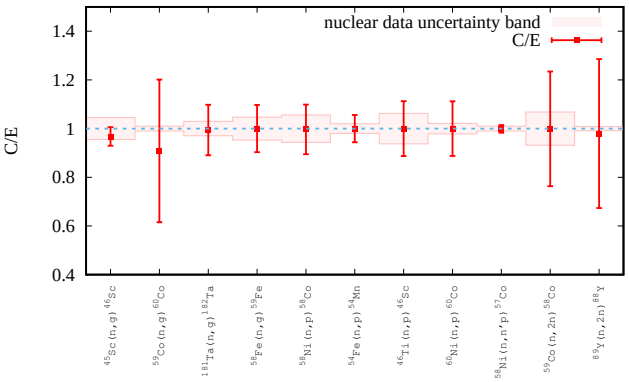

Figure 5: C/E plot for all 11 reactions measured during the experimental campaign using the final spectrum. The error bars are the combined measurement uncertainty for each reaction type. The uncertainty band shown is the nuclear data uncertainty for each reaction.

an initial MCNP calculated 'a priori' neutron spectrum, an improved spectrum. These two spectra are compared and show that the largest fluence differences are in the energy region below 2 MeV, whereas in regions at and above 2 MeV better agreement is obtained, between 8–10%. It should be noted that the uncertainty in the KN2 fission yield counter calibration, which is used here to provide the measured neutron yield as input to the initial calculation, is approximately 10%. One can therefore conclude that, within the high energy regions at least, the calculations may be regarded as consistent with experiment. Efforts under the WPJET3 project to understand which geometric features and/or materials in JET MCNP models impact on the spectrum in the 0–2 MeV are ongoing in an attempt to obtain better agreement between calculation and experiment in this energy region too.

The work presented here also demonstrates that dosimetry foil activation measurements may be used as a complimentary integrated fluence measurement system for comparison with fission neutron yield counters, such as the KN2 system used in JET, but is also highly relevant to ITER and DEMO neutron diagnostics of similar type. In addition to providing absolute measurements of neutron fluence the approach provides valuable neutron spectrum information, which has been extracted from the measurement data, particularly in energy regions above 2 MeV. The results may be used to interpret triton burn up levels for example. The spectrometry system and methodology detailed here is expected to be developed and refined further, through the upcoming JET D–D, T–T and D–T experiments and associated nuclear technology projects under WPJET3.

5. Acknowledgements

This work has been carried out within the framework of the EUROfusion Consortium and has received funding from the Euratom research and training programme 2014–2018 under grant agreement No 633053 and from the RCUK Energy Programme [grant number EP/P012450/1]. The views and opinions expressed herein do not necessarily reflect those of the European Commission.

References

[1] X. Litaudon et al, Overview of the JET results in support to ITER, Nuclear Fusion 57 (10) (2017) 102001.

[2] P. Batistoni, On the absolute calibration of neutron measurements in fusion reactors, Fusion Engineering and Design 105 (Supplement C) (2016) 58 – 69. doi:https://doi.org/10.1016/j.fusengdes.2016.02.064.
URL http://www.sciencedirect.com/science/article/pii/S0920379616301466

[3] R. Villari, P. Batistoni, M. Angelone, J. Catalan, B. Colling, D. Croft, U. Fischer, D. Flammini, A. Klix, S. Loreti, S. Lilley, F. Moro, J. Naish, L. Packer, P. Pereslavtsev, S. Popovichev, P. Sauvan, B. Syme, Neutronics experiments and analyses in preparation of DT operations at JET, Fusion Engineering and Design 109 (Part A) (2016) 895 – 905, proceedings of the 12th International Symposium on Fusion Nuclear Technology-12 (ISFNT-12). doi:https://doi.org/10.1016/j.fusengdes.2016.01.055.
URL http://www.sciencedirect.com/science/article/pii/S0920379616300576

[4] R. Villari, P. Batistoni, J. Catalan, B. Colling, D. Croft, U. Fischer, D. Flammini, N. Fonnesu, L. Jones, A. Klix, B. Kos, M. K?osowski, I. Kodeli, S. Loreti, F. Moro, J. Naish, B. Obryk, L. Packer, P. Pereslavtsev, R. Pilotti, S. Popovichev, P. Sauvan, I. Stamatelatos, T. Vasilopoulou, ITER oriented neutronics benchmark experiments on neutron streaming and shutdown dose rate at JET, Fusion Engineering and Designdoi:https://doi.org/10.1016/j.fusengdes.2017.03.037.
URL http://www.sciencedirect.com/science/article/pii/S0920379617302405

[5] B. Obryk, P. Batistoni, S. Conroy, B. D. Syme, S. Popovichev, I. E. Stamatelatos, T. Vasilopoulou, P. Bilski, Thermoluminescence measurements of neutron streaming through JET Torus Hall ducts, Fusion Engineering and Design 89 (9) (2014) 2235 – 2240, proceedings of the 11th International Symposium on Fusion Nuclear Technology-11 (ISFNT-11) Barcelona, Spain, 15-20 September, 2013. doi:https://doi.org/10.1016/j.fusengdes.2013.12.045.

[6] P. Batistoni, S. Conroy, S. Lilley, J. Naish, B. Obryk, S. Popovichev, I. Stamatelatos, B. Syme, T. Vasilopoulou, J. contributors, Benchmark experiments on neutron streaming through JET Torus Hall penetrations, Nuclear Fusion 55 (5) (2015) 053028.

[7] T. Vasilopoulou, I. Stamatelatos, P. Batistoni, S. Conroy, B. Obryk, S. Popovichev, D. Syme, Neutron streaming along ducts and labyrinths at the JET biological shielding: Effect of concrete composition, Radiation Physics and Chemistry 116 (Supplement C) (2015) 359 – 364, proceedings of the 9th International Topical Meeting on Industrial Radiation and Radioisotope Measurement Applications. doi:https://doi.org/10.1016/j.radphyschem.2015.04.015.

[8] B. C. Colling et al., Testing of tritium breeder blanket activation foil spectrometer during JET operations, Fusion Engineering and Design - article in press.

[9] L. Packer, P. Batistoni, B. Colling, K. Drozdowicz, S. Jednorog, M. Gilbert, E. Laszynska, D. Leichtle, J. Mietelski, M. Pillon, I. Stamatelatos, T. Vasilopoulou, A. Wjcik-Gargula, Status of ITER material activation experiments at JET, Fusion Engineering and Designdoi:https://doi.org/10.1016/j.fusengdes.2017.01.037.

[10] G. Stankunas, A. Tidikas, P. Batistoni, I. Lengar, Analysis of activation and damage of ITER material samples expected from DD/DT campaign at JET, Fusion Engineering and Designdoi:https://doi.org/10.1016/j.fusengdes.2017.07.013.

[11] L. Packer, P. Batistoni, S. Bradnam, B. Colling, S. Conroy, Z. Ghani, M. Gilbert, S. Jednorog, E. aszyska, D. Leichtle, I. Lengar, J. Mietelski, R. Misiak, C. Nobs, M. Pillon, S. Popovichev, V. Radulovi, I. Stamatelatos, T. Vasilopoulou, A. Wjcik-Gargula, J. Contributors, Activation of iter materials in jet: nuclear characterisation experiments for the long-term irradiation station, Nuclear Fusion 58 (9) (2018) 096013.
URL http://stacks.iop.org/0029-5515/58/i=9/a=096013

[12] M. Matzke, Propagation of uncertainties in unfolding procedures, Nuclear Instruments and Methods in Physics Research Section A: Accelerators, Spectrometers, Detectors and Associated Equipment 476 (1) (2002) 230 – 241, int. Workshop on Neutron Field Spectrometry in Science, Technolog y and Radiation Protection. doi:https://doi.org/10.1016/S0168-9002(01)01438-3.
URL http://www.sciencedirect.com/science/article/pii/S0168900201014383

[13] M. Matzke, Report PTB-N-19, Physikalisch-Technische Bundesanstalt, Braunschweig, 1994.

[14] W. M. McElroy et al., Report AFWL-TR-67-41, US Air Force Weapons Laboratory, 1967.

[15] S. Barros, Comparison of unfolding codes for neutron spectrometry with bonner spheres, Ra-

diation Protection Dosimetry 161 (1-4) (2014) 46 52.

[16] X-5 Monte Carlo Team, MCNP – a general purpose Monte Carlo N-Particle transport code, version 5, volume II: User's guide, los Alamos document number: LA-CP-03-0245. (2008 revision).